Journal of Associated Medical Sciences 2021; 54 (3): 78-83

JAMS
Journal of Associated Medical Sciences

Thai-Journal Citation Index Centre (TCI) & ASEAN Citation Index (ACI)

Journal of Associated Medical Sciences

Journal homepage: https://www.tci-thaijo.org/index.php/bulletinAMS/index



Effect of acquisition time on image quality and lesion detectability with ^{131}I SPECT: A phantom study

Supakiet Piasanthia[1] Putthiporn Charoenphun[1] Wirinya Saengthamchai[1] Krisanat Chuamsaamarkkee[1*]

[1]Department of Diagnostic and Therapeutic Radiology, Faculty of Medicine Ramathibodi Hospital, Mahidol University, Bangkok, Thailand

ARTICLE INFO

Article history:
Received 30 June 2021
Accepted as revised 18 August 2021
Available online 18 August 2021

Keywords:
^{131}I SPECT, lesion detectability, contrast, contrast-to-noise ratio, acquisition time

ABSTRACT

Background: One important parameter in single-photon emission computed tomography (SPECT) is the acquisition time. Longer acquisition time can reduce noise, improving image quality while patient motion might be presented.

Objectives: This study intended to examine the effect of acquisition time on qualitative and quantitative analysis of ^{131}I (Iodine-131) SPECT.

Materials and methods: A National Electrical Manufacturers Association/International Electrotechnical Commission (NEMA/IEC) phantom with a set of fillable spheres was filled with ^{131}I solution to generate two conditions: (a) hot lesion with no background and (b) hot lesion with a warm background at a ratio of 10:1. SPECT images were acquired with acquisition times per frame of 20, 30, 40, and 90 second/frame (s/f).

Results: Qualitative assessment in the no background condition showed that all spheres were visible at all acquisition settings, while the smallest sphere in the images in hot lesion with a warm background at a ratio of 10:1 was not visible even at the longest acquisition time of 90 s/f. Quantitative analysis revealed that the contrast and contrast-to-noise ratio (CNR) increased upon extending the acquisition time in both conditions. Interestingly, the statistical results indicated that the mean CNRs acquired at 20 or 30 s/f were not significantly different when compared with 40 s/f for no background. However, for the warm background, the mean CNRs at 20 s/f were significantly different than those at 40 s/f, while they were not significantly different at 30 s/f.

Conclusion: The acquisition time for no background condition can be optimized, while the image quality is still clinically acceptable. For the warm background, the acquisition time can be shortened; however, the time selection must be carefully considered.

Introduction

Radioiodine (^{131}I) has been used for the diagnosis and treatment of thyroid diseases for over 80 years. The beta emissions offer a therapeutic property whereas the discrete gamma photons can be imaged with nuclear medicine imaging techniques to provide clinical information such as tumour size, treatment efficiency, sites of metastasis, and dosimetry calculations.[1, 2]

For many decades, the whole-body planar imaging of ^{131}I was the standard method used to identify the thyroid remnant, metastases, or lesion. However, low resolution and lack of anatomical localization make interpretation of ^{131}I planar imaging challenging. Several recent studies suggested that ^{131}I SPECT provides superior clinical results compared to ^{131}I planar imaging.[3-5] Nonetheless, undesirable

* **Corresponding author.**
Author's Address: *Department of Diagnostic and Therapeutic Radiology, Faculty of Medicine Ramathibodi Hospital, Mahidol University, Bangkok, Thailand.*
** **E-mail address:** krisanat.chu@mahidol.ac.th
doi: 10.14456/jams.2021.27
E-ISSN: 2539-6056

image quality with ^{131}I could compromise the accuracy and detectability limit.[6, 7] One important parameter in SPECT is the acquisition time, which refers to the time per stop in the imaging parameter. Unquestionably, longer acquisition time has the advantages of higher counts, noise reduction, as well as better contrast and resolution. On the other hand, longer acquisition time can be associated with patient agitation that can further result in artefacts and image degradation.[8, 9]

Although several studies have attempted to study the clinical impact of acquisition time reduction using resolution recovery software in bone and parathyroid SPECT with Technetium-99m.[10, 11] Nevertheless, fewer studies have attempted to study with ^{131}I SPECT due to the complexity of its emission spectrum. Therefore, this study intended to examine the effect of acquisition time on image quality and aimed to qualitatively assess this effect on lesion detectability with ^{131}I SPECT using NEMA/IEC (National Electrical Manufacturers Association/International Electrotechnical Commission) body phantom.

Materials and methods

Phantom preparation

The NEMA/IEC body phantom (Data Spectrum Corp., Chapel Hill, North Carolina, USA) with a set of fillable hollow spheres was used in this study. The volume and inner diameter (ID) of the fillable hollow spheres were 26.52 mL (ID 37 mm), 11.49 mL (ID 28 mm), 5.58 mL (ID 22 mm), 2.57 mL (ID 17 mm), 1.15 mL (ID 13 mm), and 0.52 mL (ID 10 mm). However, the 5.58 mL sphere was excluded from the experiment due to a defect. The spheres were filled with an aqueous solution of ^{131}I-sodium iodide (NaI) with an activity concentration of 740 kBq.mL^{-1} to simulate a hot lesion. The background activity was filled with deionized water and ^{131}I-NaI with an activity concentration of 74 kBq.mL^{-1} to simulate no background and the hot lesion to warm background ratio of 10:1, respectively. The selected concentration was based on ^{131}I clinical images from previously published studies.[12-14]

SPECT scanner and acquisitions

All SPECT images were acquired using a dual-head gamma camera (Infinia Hawkeye-4, General Electric Medical Systems, Milwaukee, Wisconsin, USA) equipped with a high-energy general purpose (HEGP) collimator and crystal thickness of 25.4 mm. The projection data were acquired for 60 views with 360° camera rotation in the orbit mode. The main photo peak was set at 364 keV and 20% energy window. The acquisition time per frame was varied from 20, 30, 40, and 90 s/f. Additional CT images were also acquired for localization of the hot spheres.

Image reconstruction

All SPECT data were reconstructed with the ordered subsets expectation maximization (OSEM) method (2 iterations and 10 subsets per series) and a Hann filter, as recommended by the manufacturer. Image size was 128 × 128 and the slice thickness was 4 mm. The attenuation correction was performed with Chang's method. The scatter correction was also carried out using the dual-energy window method with a lower scatter window set at 297 keV with 20% energy window).

Qualitative analysis

To perform qualitative analysis, all SPECT images were analysed by a consensus between three nuclear medicine physicians (each with at least 3 years of experience). The subsequent images were blindly graded by each observer; "S" was given when the sphere was observed, and "NS" was given when the sphere was not observed. The final qualitative evaluation for each sphere was based on a consensus between at least 2 out of the 3 observers.[15] Cohen's kappa (k) statistic was used to assess agreement between the observers.[16]

Quantitative analysis

For quantitative analysis, we calculated contrast and contrast-to-noise ratio (CNR) for each sphere using equations 1 and 2.[14]

$$contrast = \frac{|C - C_B|}{C_B} \quad (1)$$

$$CNR = \frac{|C - C_B|}{\sigma_B} \quad (2)$$

where C is the mean pixel value in the sphere region of interest (ROI), C_B is the mean voxel value in the background ROI, and σ_B is the standard deviation (SD) in the background ROI. Then, ROIs were created and positioned on the co-registered CT image with the size being about 50% of each sphere. The background ROI was delineated at the center of the phantom. To eliminate inconsistency, the ROIs were repeatedly drawn on three separate occasions. The mean CNRs and SDs were calculated (mean±SD) and plotted. A two-tailed, paired student t-test was used to determine statistical significance by setting the probability (p=0.05, 95% confidence interval).

Results

Based on our experiments, Figure 1 shows the sample of selected transverse (axial) images of the NEMA IEC body phantom for different acquisition times per frame of the hot lesion with no background (row A) and the hot lesion with a warm background at a ratio of 10:1 (row B).

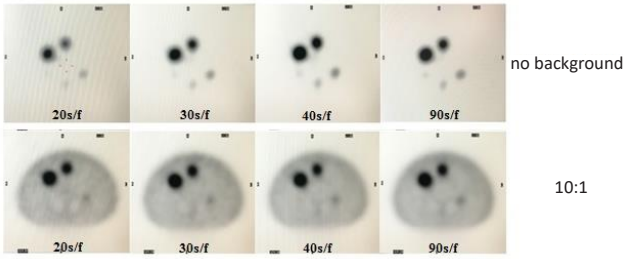


Figure 1. *Examples of selected transverse (axial) images of the NEMA/IEC (National Electrical Manufacturers Association/International Electrotechnical Commission) body phantom with (a) hot lesion with no background and (b) hot lesion with warm background at a ratio of 10:1, with acquisition times at 20, 30, 40, and 90 s/f.*

The qualitative results after consensus from three experienced nuclear medicine physicians are tabulated in Table 1. For hot lesions with no background, all spheres were observed at every acquisition time. In contrast, the smallest sphere (0.52 mL, ID 10 mm) was not seen even with the longest acquisition of 90 s/f for hot lesions with a warm background at a ratio of 10:1.

Table 1 Qualitative result (consensus from 2 out of 3 observers).

	Acquisition time (time per frame)							
	20 s		30 s		40 s		90 s	
Volume (mL)	NB[a]	10:1[b]	NB[a]	10:1[b]	NB[a]	10:1[b]	NB[a]	10:1[b]
26.52	S	S	S	S	S	S	S	S
11.49	S	S	S	S	S	S	S	S
2.57	S	S	S	S	S	S	S	S
1.15	S	S	S	S	S	S	S	S
0.52	S	NS	S	NS	S	NS	S	NS

[a]*NB: hot lesion with no background,* [b]*10:1: hot lesion with a warm background at a ratio of 10:1.*

For quantitative analysis, effects of acquisition time on image contrast (mean±SD) for each sphere are presented in Figure 2. The contrast decreased as the acquisition time shortened. The highest contrast was observed when setting the acquisition time 90 s/f and the larger sphere presented with greater contrast as expected. For hot lesions with no background, the image contrast for small spheres (0.52 mL, 1.15 mL, and 2.57 mL) of 30 and 40 s/f acquisitions were oscillated, which is further discussed in the following section. The image contrast for lesion to background ratio 10:1 for all spheres were as anticipated.

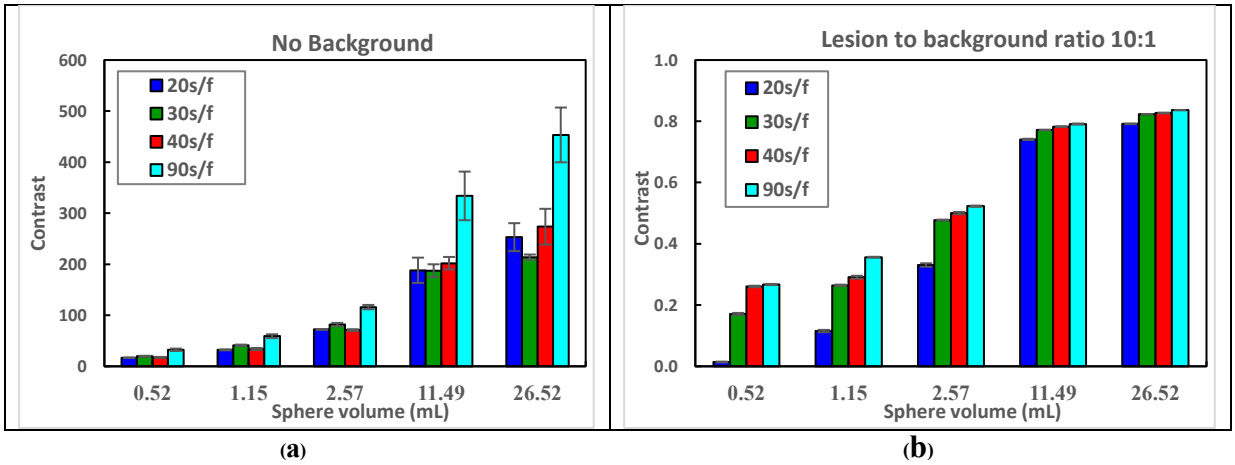


Figure 2. *Image contrast (mean±SD) plot with sphere sizes. The blue, green, red, and light blue represent acquisition times at 20, 30, 40, and 90 s/f. (a): hot lesion with o background, (b): hot lesion with a warm background at a ratio of 10:1.*

The plot of CNR (mean±SD) for each sphere volume as a function of acquisition time per frame is shown in Figure 3. As expected, the highest CNR was found when scanning with 90 s/f for both conditions. For the hot lesion with no background, the CNRs increased when acquisition time was prolonged, especially in large spheres (sizes of 11.49 and 26.52 mL). For the hot lesion with a warm background at a ratio of 10:1, the mean CNRs also increased when acquisition time was increased; interestingly, these longer acquisition times had a greater effect on CNR compared with the hot lesion with no background.

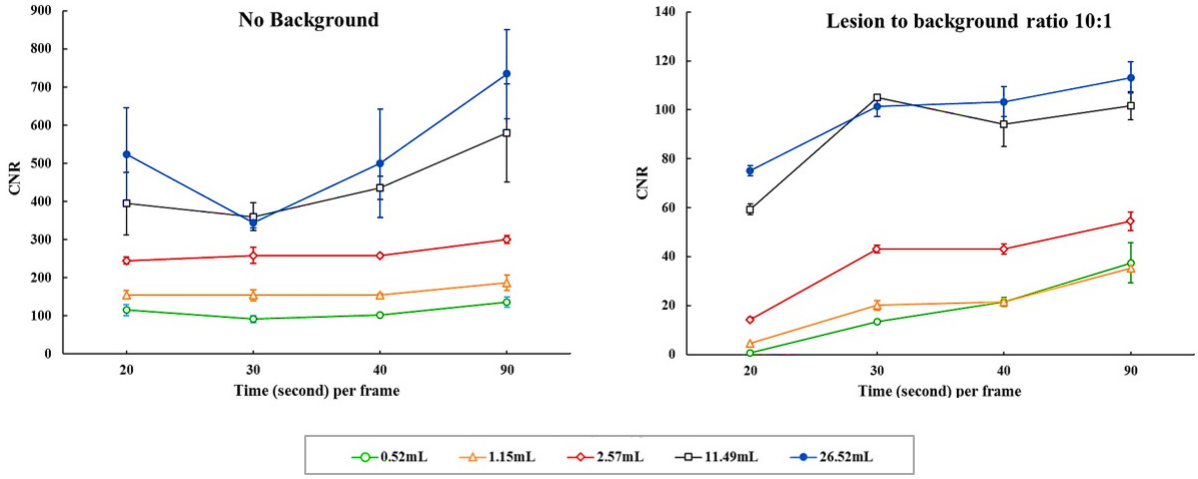


Figure 3. *Quantitative contrast-to-noise ratio (CNR) analysis (mean±SD) plot with acquisition time (time per frame). (a) hot lesion with no background and (b) hot lesion with a warm background at a ratio of 10:1.*

Additionally, the statistical results of ^{131}I quantification are presented in Table 2. Here, the mean CNR of acquisition time at 40 s/f (our clinical setting) was used as a standard to compare with other data sets. The data were considered statistically significant when $p<0.5$.

Table 2 Statistical results of ^{131}I quantitative evaluation.

	Statistical Results (time per frame)[a]					
	20 second		30 second		90 second	
Volume (mL)	NoBkg	10:1	NoBkg	10:1	NoBkg	10:1
26.52	Y	X(p=0.0173)	Y	Y	Y	Y
11.49	Y	X(p=0.0242)	Y	Y	Y	Y
2.57	Y	X(p=0.0020)	Y	Y	X(p=0.0067)	X(p=0.0194)
1.15	Y	X(p=0.0060)	Y	Y	Y	X(p=0.0004)
0.52	Y	X(p=0.0025)	Y	X(p=0.0178)	Y	Y

[a]*X: significant differences (p<0.05), Y: not significantly different.*

The statistical results for the hot lesion with no background indicate that mean CNRs for acquisition times at 20 and 30 s/f were similar to that at 40 s/f. Meanwhile, the CNR for the 2.5-mL sphere was statistically different at 90 s/f (p=0.0067). For the hot lesion with a warm background at a ratio of 10:1, the mean CNRs for all spheres acquired at 20 s/f were statistically different from those at 40 s/f. Significant results were also found in the smallest sphere (0.52 mL) at 30 s/f, and in the 1.15- and 2.57-mL spheres at 90 s/f.

Discussion

The qualitative performance of SPECT imaging was evaluated by three experienced nuclear medicine physicians. For infinite contrast (no background), all volume sizes of the spheres (0.52 to 26.52 mL) were detected at all acquisition times (20, 30, 40, and 90 s/f). This agrees well with the published work by Erdi, who also reported the detectability limit of radioiodine with SPECT at a tumour diameter of about 1 cm (volume about 0.53 mL).[17]

For hot lesion with a warm background at a ratio of 10:1, this ratio was typically found in clinical studies such as ^{131}I-metaiodobenzylguanidine (mIBG) for tumour imaging.[12] Our qualitative results indicate that the nuclear medicine physicians could not detect the smallest sphere of 0.52 mL. As the consensus result was used to evaluate the same set of SPECT images, consequently, the inter-observer and Kappa agreement were also analysed (as tabulated in Table 3).

Table3 Kappa analysis for inter-observer agreement.

Observer[a]	Percentage Observed Agreement	Kappa Agreement (K)	Interpretation [b]
Observer 1 vs. Observer 2	100.00	1.000	Perfect Agreement
Observer 1 vs. Observer 3	87.50	0.479	Moderate Agreement
Observer 2 vs. Observer 3	87.50	0.479	

[a]*observer 1, observer 2, and observer 3 have work experience of 7, 6, and 4 years, respectively,* [b]*Interpretation of kappa is based on published work by Viera AJ and Garrett JM.*

Based on Table 3, the agreement between observers 1 and 2 (K=1.000) was higher than that between observers 1 and 3 (K=0.479), and that between observers 2 and 3 (K=0.479). Despite having at least 3 years of experience, the differences between their years of experience have been clearly demonstrated in this study as the agreement was higher and more consistent for the more experienced observer. Hence, this can be noted as one of the limitations of this study.

In this study, the effect of acquisition time on quantitative detectability was examined using contrast and CNR. Contrast is related to diameter of sphere, uptake ratio, and resolution of imaging system. The measured contrast decreased when the acquisition time was shortened. Additionally, the contrast detail was inferior in the small spheres. This might have resulted from the partial volume effect (PVE), which is related to poor resolution of imaging systems and usually results in underestimating the activity. Many published works suggest that the object size must be larger than 2 times the system's full-width at half maximum (FWHM) to avoid PVEs.[18-20] The Medical Internal Radiation Dose (MIRD) pamphlet no.24: *Guidelines for quantitative ^{131}I SPECT in dosimetry applications* recommended that PVEs due to poor resolution of ^{131}I SPECT can be observed for any volumes that are smaller than approximately 8 mL (about 25 mm diameter).[21] Hence, according to the IEC phantom specification, only the 26.52 mL-spheres (37 mm diameter) and 11.49 mL-spheres (28 mm diameter) did not suffer from PVEs.

Imaging performance in terms of contrast and CNR was investigated in this work. As a rule of thumb, contrast increases with longer acquisition times due to higher count levels. Additionally, contrast in larger spheres is greater than that in smaller spheres, which also result in a loss in count signal from the PVE as described above. However, it

would be more representative to consider the noise component based on CNR, rather than only raw contrast signal. For the phantom with hot lesion without activity in the background, the mean CNRs improved with increased acquisition times. This result agreed well with those presented by M Elschot *et al*., who remarked that the CNR in hot spots was related to the number of counts in the region.[22] Furthermore, a recent study by M Brambilla *et al*. also demonstrated that contrast or CNR is associated with the number of counts in the data set.[23] Their result indicated that low counts lead to higher levels of deviation and non-Poisson statistics, which may reduce the CNR and quantitative accuracy. This is evident by the relatively high standard deviation of the analysed contrast and CNR as shown in Figure 2 and 3 in the short acquisition time.

Regarding the effects of sphere size, larger spheres were found to have higher CNRs compared to smaller spheres. This also resulted from a loss in count signal for objects with diameters that are small or similar in size to the resolution of the system. For the condition of lesion to background ratio of 10:1, the mean CNRs for each sphere were decreased compared to those with no background conditions. In this study, the ROI was fixed with the size of about half of the diameter of each sphere, using CT data as a guide for the ROI location. This helped to minimize the counts from background activity. However, the decrease in CNR also resulted from elevated background radiation from the scattered ^{131}I photons.

From the two-tailed, paired student t-test statistical analysis as tabulated in Table 2, there was no statistical significance between mean CNRs when acquired at 20 and 30 s/f for all sphere sizes compared to our clinical practice (40 s/f) when no background activity was present. Nevertheless, mean CNR of 2.57-mL sphere acquired with 90 s/f was statistically significant (p=0.0067), while larger and smaller spheres were not statistically different in the no background condition. However, these results included a large SD from drawing ROIs in the background region. This could be due to the scattered photons as we observed that background noises were higher in the no background condition than that of hot lesion with a warm background at a ratio of 10:1. On the other hand, for the hot lesion with a warm background at a ratio of 10:1, mean CNRs acquired at 20 s/f were significantly different from our current clinical practice for all sphere sizes. In addition, the statistical result indicates that only the mean CNR of the smallest sphere (0.52 mL) significantly differed when acquired at 30 s/f, while the other spheres presented no difference. This indicates that the acquisition time per frame must be carefully considered when the lesions are small and background activity is present. At 90 s/f, the results were undersigned as the mean CNRs of the 1.15 mL- and 2.57-mL spheres were not statistically significant while the other spheres (0.52, 11.49, and 26.52 mL) presented no difference. This error might explain the experimental error of CNR at 90 s/f. Hence, repeating this experiment is required for further study.

Furthermore, the main limitation of this work is that the data were only generated from a phantom, which is not sufficient for an actual clinical situation in terms of exact organ shape, non-uniform distribution, and the activity concentration in the organ. For the latter factor, the simulated concentration of 740 kBq/mL in our study did not cover all ^{131}I concentrations in clinical practice. However, the data may provide an idea of the method to determine the effects of acquisition time and lesion detectability. Additionally, this work was studied on a 25.4 mm (1 inch) thick crystal SPECT system. Data obtained with a standard 9.5 mm (3/8 inch) thick crystal could have resulted in lower efficiency. However, the clinical impact of this study has demonstrated that it is possible to reduce the total scanning time and the image quality is still clinically acceptable. This can reduce motion artefacts due to long scanning times. Moreover, this work has provided a study model to extend this qualitative and quantitative analysis to optimize other related factors, such as reconstruction parameters and other scatter modelling methods for lesion detectability with ^{131}I SPECT.

Conclusion

The effect of acquisition time on image quality and lesion detectability of 131I SPECT was quantitatively and qualitatively analysed using NEMA/IEC phantom. The clinical impact of this study could be shortening total scan time by determining the lesion size and background activity from the whole-body image prior to SPECT. For no background condition, the acquisition time could be set at 20 or 30 s/f (instead of 40 s/f), which led to reducing 5 to 10 minutes of total acquisition time. Based on our results, there was no statistically significant difference in terms of CNR when compared with 40 s/f, as well as with qualitative assessment by experienced observers. For the lesion with a warm background at a ratio of 10:1, the reduction is possible. However, the size of the lesion should be considered, especially when the lesions are small.

Conflict of interest

The authors declare that they have no conflicts of interest.

Ethic approval

This article does not contain any studies performed with human participants and animals.

References

[1] Xue Y-L, Qiu Z-L, Perotti G, Salvatori M, Luo Q-Y. 131I SPECT/CT: a one-station imaging modality in the management of differentiated thyroid cancer. Clin Transl Imaging. 2013; 1(3): 163-73.

[2] Salvatori M, Perotti G, Villani MF, Mazza R, Maussier ML, Indovina L, et al. Determining the appropriate time of execution of an I-131 post-therapy whole-body scan: comparison between early and late imaging. Nucl Med Commun. 2013; 34(9): 900-8.

[3] Beijst C, Kist JW, Elschot M, Viergever MA, Hoekstra OS, de Keizer B, et al. Quantitative Comparison of 124I PET/CT and 131I SPECT/CT Detectability. J Nucl Med. 2016; 57(1): 103-8.

[4] Kenneth FK, Anastasia Y, Yuni KD. Recovery of total I-131 activity within focal volumes using SPECT and 3D OSEM. Phys Med Biol. 2007;52(3): 777.

[5] Rault E, Vandenberghe S, Van Holen R, De Beenhouwer J, Staelens S, Lemahieu I. Comparison of image quality of different iodine isotopes (I-123, I-124, and I-131). Cancer Biother Radiopharm. 2007; 22(3): 423-30.

[6] Oh JR, Byun BH, Hong SP, Chong A, Kim J, Yoo SW, et al. Comparison of (1)(3)(1)I whole-body imaging, (1)(3)(1)I SPECT/CT, and (1)(8)F-FDG PET/CT in the detection of metastatic thyroid cancer. Eur J Nucl Med Mol Imaging. 2011; 38(8): 1459-68.

[7] Radioiodine Scintigraphy with SPECT/CT: an Important diagnostic tool for thyroid cancer staging and risk stratification. J Nucl Med. 2012;53(5): 754-64.

[8] He B, Frey EC. Effects of shortened acquisition time on accuracy and precision of quantitative estimates of organ activity. Med phys. 2010; 37(4): 1807-15.

[9] Bar R, Przewloka K, Karry R, Frenkel A, Golz A, Keidar Z. Half-time SPECT acquisition with resolution recovery for Tc-MIBI SPECT imaging in the assessment of hyperparathyroidism. Mol Imaging Biol. 2012; 14(5): 647-51.

[10] Aldridge MD, Waddington WW, Dickson JC, Prakash V, Ell PJ, Bomanji JB. Clinical evaluation of reducing acquisition time on single-photon emission computed tomography image quality using proprietary resolution recovery software. Nucl Med Commun. 2013; 34(11): 1116-23.

[11] Thientunyakit T, Taerakul T, Chaudakshetrin P, Ubolnuch K, Sirithongjak K. A comparison of the diagnostic performance of half-time SPECT and multiplanar pelvic bone scan in patients with significant bladder artifacts. Nucl Med Commun communications. 2013; 34(3): 233-9.

[12] Tan HK, Wassenaar RW, Zeng W. Collimator selection, acquisition speed, and visual assessment of 131I-tositumomab biodistribution in a phantom model. J Nucl Med Technol. 2006; 34(4): 224-7.

[13] Pereira JM, Stabin MG, Lima FRA, Guimarães M, Forrester JW. Image quantification for radiation dose calculations – limitations and uncertainties. Health phy. 2010; 99(5): 688-701.

[14] Van Gils CA, Beijst C, Van Rooij R, De Jong HW. Impact of reconstruction parameters on quantitative I-131 SPECT. Phys Med Biol. 2016; 61(14): 5166-82.

[15] Trägårdh E, Johansson L, Olofsson C, Valind S, Edenbrandt L. Nuclear medicine technologists are able to accurately determine when a myocardial perfusion rest study is necessary. BMC Med Inform Decis Mak. 2012; 12(1): 97.

[16] Viera AJ, Garrett JM. Understanding interobserver agreement: the kappa statistic. Fam Med. 2005; 37(5): 360-3.

[17] Erdi YE. Limits of tumor detectability in nuclear medicine and PET. Mol Imaging Radionucl Ther. 2012; 21(1): 23.

[18] Kessler RM, Ellis JR, Jr., Eden M. Analysis of emission tomographic scan data: limitations imposed by resolution and background. J Comput Assist Tomogr. 1984; 8(3): 514-22.

[19] Zaidi H. Quantitative Analysis in Nuclear Medicine Imaging: Springer US; 2006.

[20] Burg S, Dupas A, Stute S, Dieudonné A, Huet P, Guludec DL, et al. Partial volume effect estimation and correction in the aortic vascular wall in PET imaging. Phys Med Biol. 2013; 58(21): 7527.

[21] Dewaraja YK, Ljungberg M, Green AJ, Zanzonico PB, Frey EC, Bolch WE, et al. MIRD pamphlet No. 24: Guidelines for quantitative 131I SPECT in dosimetry applications. J Nucl Med. 2013; 54(12): 2182-8.

[22] Elschot M, Vermolen BJ, Lam MG, de Keizer B, van den Bosch MA, de Jong HW. Quantitative comparison of PET and Bremsstrahlung SPECT for imaging the in vivo yttrium-90 microsphere distribution after liver radioembolization. PLoS One. 2013; 8(2): e55742.

[23] Brambilla M. Performance evaluation of hardware and software for spect cardiac imaging. Physica Medica. 2016; 32, Supplement 3: 179.